

# A semi-autonomous adaptive impedance grip force controller for teleoperated object grasping

Marlies Popken



# A semi-autonomous adaptive impedance grip force controller for teleoperated object grasping

by

to obtain the degree of Master of Science  
at Delft University of Technology  
to be defended on February 24th 2023.

Student number: 4568400  
Master Program: Robotics  
Thesis committee: Dr. L. Peternel TU Delft, supervisor, chair  
Dr. M. Wiertelwski TU Delft, supervisor  
Dr. J. Kober TU Delft, external committee member



An electronic version of this thesis is available at <http://repository.tudelft.nl/>.



# A semi-autonomous adaptive impedance grip force controller for teleoperated object grasping

Marlies Popken

supervised by Michaël Wiertlewski and Luka Peternel

**Abstract**—While defusing a bomb or performing a rescue mission with a teleoperated robot, grasping various objects is crucial. Despite being a routine activity, remote grasping is still challenging. It is difficult to apply an adequate grip force to avoid slippage and damage to an object. An additional challenge is controlling both motion and force at the same time during remote robot control (teleoperation). Therefore, this research presents a teleoperated semi-autonomous controller which assists the user with remote grasping by relieving the user from controlling the grip force. Our design enables the user (1) to control the position of the remote gripper while (2) the system controls the grip force autonomously. When the user grasps an object, the semi-autonomous controller maintains the grip force based on tactile feedback to prevent object slippage. For tactile feedback, our system uses a tactile sensor that can detect incipient slippage from deformations at the location of the contact. With two experiments, we show that the system can maintain an adequate grip force while being robust to external perturbations and input changes. Since this controller stably grasps objects while the user maintains control over the position of the remote robot, our method relieves the user and prevents object slippage.

**Index Terms**—teleoperation, adaptive impedance, semi-autonomous, grip force, grasping.

## 1 INTRODUCTION

Robots can operate in places that humans cannot reach. They perform tasks in outer space [1], [2] or reach disaster areas for search and rescue missions [3]–[5], protecting humans from dangerous situations. Most of the time, these robots cannot accomplish a task independently and must be remotely controlled. Teleoperation, a local-remote robot device, allows for remote robot control. It enables a robot to perform a task with the expertise of a human as the user controls the remote robot with a local interface. This way, the user is not physically present at the remote device, which enables the user to defuse bombs and rescue people safely. [6]–[8].

Object grasping is essential for the successful execution of a task, such as defusing a bomb or rescuing people. However, the user is limited while grasping with a teleoperated device (tele-grasping). The user cannot determine the necessary force to apply due to the lack of physical contact with the grasped object. This can lead to applying too much force and damaging the object, or too little force, causing it to slip.

Grasping objects is difficult with teleoperated robots, but when humans grasp themselves they grasp objects precisely due to their sense of touch. Humans can predict the required grip force based on object properties and previous experiences [9], [10]. Additionally, they use their dexterity to minimize the impact while establishing contact with an object [11], [12]. When contact is established, humans apply a grip force that causes grasp stability. Grasp stability is “The control of grip forces such that they are adequate to prevent accidental slips but not so large that they cause unnecessary fatigue or damage to the object or hand.” as defined by Johansson et al [9]. This means that the grip force applied for a stable grasp is more than the minimum required grip force, but not an excessive amount. To maintain grasp stability, humans apply 10 - 40 % more grip force than the minimal

required, also called the grip force safety margin [9].

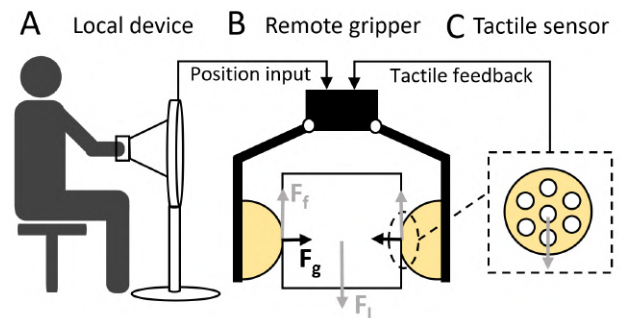


Fig. 1: This figure shows the semi-autonomous adaptive impedance grip force controller on a tele-grasping device. The grip force is based on both the commanded position of the user and tactile feedback. **A)** The user controls the local device to command the desired position. **B)** The grip force applied by the remote gripper is computed based on the commanded position and tactile feedback. The forces between the object and the gripper are also visualized:  $F_g$  is the grip force,  $F_f$  is the friction force, and  $F_l$  is the load force of the object **C)** Tactile feedback is computed based on deformations in the contact area between the object and the gripper caused by incipient slip.

Humans grasp objects with their hands, whereas in tele-grasping, the user controls a remote device to grasp an object without physically touching it. This stops the user from using his sense of touch while controlling the remote robot to estimate the appropriate grip force. However, the ability to adjust the grip force remotely depends on the implemented tele-grasping controller.

Currently, teleoperated control methods can be categorized into three groups: position [13], [14], force [13], [15]

and impedance control[16]–[22]. For grasping, these control methods have different qualities. A position controller copies the commanded position at the local device to the remote robot. The controller at the remote robot will apply as much force as needed to reach the commanded position. Since the position controller only cares about reaching the desired position, this could cause high-impact forces on the object and potential damage if the position commands are inaccurate. For example, an operator commands the remote gripper to grasp a glass and sets a target position inside the object. High forces will be applied to reach that position, resulting in a high-impact force on the glass surface and potential damage.

The opposite of a position controller is a force controller. A force controller copies the commanded force at the local device to the remote gripper. The controller at the remote robot will apply the commanded force independent of the gripper’s position. If the commanded force is too high, it could cause high-impact forces on the object and cause damage. If the force is too low, it could cause the object to slip. For example, to grasp a banana, a user commands on the local device a force to close the remote gripper. The gripper will close with the desired force. However, if the commanded force is too low, the banana will slip out of the gripper and fall to the ground.

An impedance controller differs from a position and force controller. While a position controller does not care about the force, and a force controller does not care about the position, an impedance controller controls the relation between position and force. The user commands a position at the local device, which is compared to the position of the remote gripper. The difference in position scales with impedance properties the force at the remote gripper to move towards the desired position. This enables the user to control the position of the remote gripper and the impact force while grasping an object. For example, when an operator teleoperates a gripper to grasp a cup, the impact force is reduced if the impedance properties are set low. This allows the user to handle objects without causing damage. Because an impedance controller allows for better control of the interaction between the gripper and the object, it is the preferred controller for tele-grasping compared to position and force control.

During impedance control, the user controls the force by adapting the difference in position between the commanded and the robot’s actual position. To improve the adaptability of the remote force, the impedance properties of the controller can be adapted during the task. An impedance controller with variable impedance properties is called an adaptive impedance controller.

Current state-of-the-art adaptive impedance methods enable the user to adapt the impedance properties with an external device[23]–[25], muscle activity[26], [27] or by posture tracking of the user [26]. But, all these methods require effort from the user. To relieve the user, Brygo et al. implemented an autonomous impedance property controller. This controller adjusts impedance properties based on the external load force at the robot’s end effector to control the grip force. By implementing an autonomous impedance property controller in an adaptive impedance method, the user can entirely focus on controlling the position [28].

However, the autonomous impedance property controller does not ensure that the applied grip force is equivalent to the one guaranteeing grasp stability. To address this gap, we propose a semi-autonomous controller for tele-grasping. With this controller, the user maintains the ability to command the desired gripper position. While an autonomous impedance property controller ensures grasp stability. A schematic overview can be seen in Fig. 1. This method should enable two objectives (1) the user controls the position of the remote gripper, and (2) the grip force is controlled autonomously to maintain grasp stability. More details about this controller are described in Section 3. To test the controller, we implemented it on a tele-grasping device. This device consists of a local gripper controlled by the user and a remote robot. The remote robot is a gripper mounted on a manipulator to increase the degrees of freedom. We performed two experiments to test the controller’s performance. The experiments, *adaptability to external changes* and *adaptability to human input* test the controller during load force changes and user input perturbations. In addition, the experiments are also conducted with a force and impedance controller for a supplementary comparison, see Section 4. The results show that the controller maintains grasp stability and is discussed in Section 5 and 6, respectively.

## 2 BACKGROUND

Before we explore the method of our designed controller, it is necessary to understand how we can measure grasp stability based on the grip force safety margin. To maintain grasp stability, humans apply 10 - 40 % more grip force than the minimum required. This additional amount of force is called the grip force safety margin. To determine the safety margin, the minimal required grip force must be known, which depends on the lateral force and the coefficient of friction of the grasped object (Equation 1). However, detecting the coefficient of friction for every grasped object is inconvenient. Therefore, Boonstra proposed computing the safety margin based on the frictional state of the object [29]. Instead of viewing the safety margin as an additional force that prevents object slippage, they approach the safety margin as an estimate of how close an object is to slippage.

There is no slippage as long as static friction is present between the object and the gripper. As there is no slip, the safety margin is  $> 0$ .

$$F_l \leq \mu_s F_{grip} \quad (1)$$

With  $F_l$  the lateral force,  $\mu_s$  the static coefficient of friction, and  $F_{grip}$  the grip force.

An object starts to slip when kinetic friction occurs. The safety margin, in this case, equals 0.

$$F_l^* = \mu_k F_{grip} \quad (2)$$

With  $F_l^*$  the critical lateral force,  $\mu_k$  the kinetic coefficient of friction, and  $F_{grip}$  the grip force.

The critical lateral force ( $F_l^*$ ) is thus the force above which slippage occurs. As long as  $F_l < F_l^*$ , the object is not slipping. Based on this difference between the lateral force and the critical lateral force, the safety margin ( $\Gamma$ ) is computed [29].

$$\Gamma = 1 - \frac{F_l}{F_l^*} \quad (3)$$

Another method to compute the safety margin is based on deformations in the contact surface between the object and the gripper. Deformations emerge due to indentation, shear stress and slippage. Given that the safety margin, as defined in Equation 3, estimates slippage. We could also estimate slippage by analysing deformations which occur before slip.

Slippage causes distinctive deformations in the contact surface, but to explain these, we first have to clarify the different phases of slip. Until now, we used the word slippage to indicate that an object shows displacement relative to the grasping medium. However, slippage consists of two stages, incipient slip and gross slip. When there is relative displacement, the object is already in the second stage, gross slip.

During incipient slip, the contact area between the gripper and the object deforms and detaches from the object in the peripheral area of the contact surface, causing slippage in the outer area of the contact surface. Despite this, there is no relative movement because the centre of the contact area remains in contact with the object, which can withhold the lateral force. As incipient slip increases, the detachments move towards the centre of the contact area. When the contact area cannot withhold the lateral force anymore, the entire area detaches, and gross slippage occurs (Fig. 2).

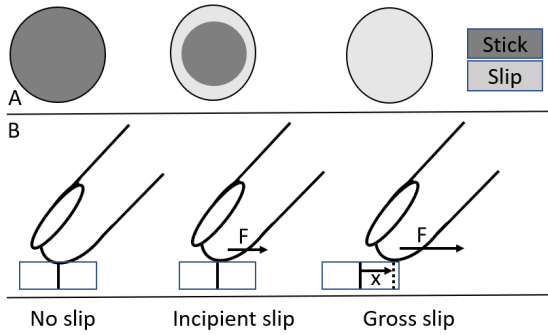


Fig. 2: Stages of slip between a fingertip and an object. **A)** The stick-slip ratio in the contact surface. **B)** The displacement and the force exerted by a fingertip

The deformations caused by incipient slip represent how close gross slippage is and thus can be used as an input to compute the safety margin. Boonstra proved that safety margin predictions based on deformations is possible. They captured the deformation caused by incipient slip in an image as an input for a neural network to compute the safety margin [29]. However, this method has two disadvantages. It has a low prediction frequency and demands a large data set for training, which is inconvenient as we want to use it as an input for our controller. To improve this method, we implement in this research a numerical implementation to increase the prediction frequency and reduce the need for prior training. We elaborate on this in Section 3.1.

### 3 METHODOLOGY

In this research, we introduce a semi-autonomous adaptive impedance controller for tele-grasping, allowing the user to control the position of the remote gripper while the grip force is controlled autonomously to maintain grasp stability. The system consists of four parts: The safety margin detector (Section 3.1), the adaptive impedance controller (Section 3.2), the impedance property controller (Section 3.3) and feedback (Section 3.4), as illustrated in Fig. 3. The adaptive impedance controller is the system's foundation, enabling the user to control the position of the remote gripper even though the remote robot is controlled by forces. The force at the remote gripper is regulated by the impedance property controller, which adjusts the damping and stiffness term to fit the task. During grasping, the impedance properties enable grasp stability, while during non-grasping tasks, the remote gripper is compliant. The impedance property controller relies on the safety margin as an input to maintain grasp stability. Therefore a safety margin detector is used. Feedback is present to inform the user when contact is made with an object.

#### 3.1 Safety margin detection

The safety margin is an estimation of the proximity of gross slip. This margin is determined by tracking the deformations in the contact area between the grasped object and the gripper. As incipient slip occurs, deformations arise in the contact surface. These deformations grow larger when incipient slip increases, as less contact surface sticks to the object. Moments before gross slippage takes place, the deformations are at their maximum. This enables us to compute the safety margin ( $\Gamma$ ) with Equation 4.

$$\Gamma = 1 - \frac{\delta}{\delta^*} \quad (4)$$

with  $\delta$  the measured deformation, and  $\delta^*$  the critical deformation. The critical deformation is the deformation at which the object is on the verge of gross slippage. The critical deformation depends on the grip force and the material of the grasped object. Therefore, every object has a set of critical deformations which correspond with different grip forces.

The safety margin, relative to the deformation in the contact surface, is visualized in Fig. 4. The safety margin is 0 when  $\delta = \delta^*$ , the object is on the verge of gross slippage. When  $\delta < \delta^*$  the safety margin is between 0 and 100. If we desire a safety margin of approximately 30%, the grip force should be adapted to fit a deformation which corresponds with the reference safety margin.

Detecting deformations with sensors is difficult, as a minimal force is required to detect deformations. Therefore we include a minimal grip force ( $F_{min}$ ) in the controller. If the force of the impedance controller does not exceed this threshold while deformations are detected, the force will be overwritten.

$$F_{gripper} = \begin{cases} F_{min}, & \text{if } F < F_{min} \\ F, & \text{otherwise} \end{cases} \quad (5)$$

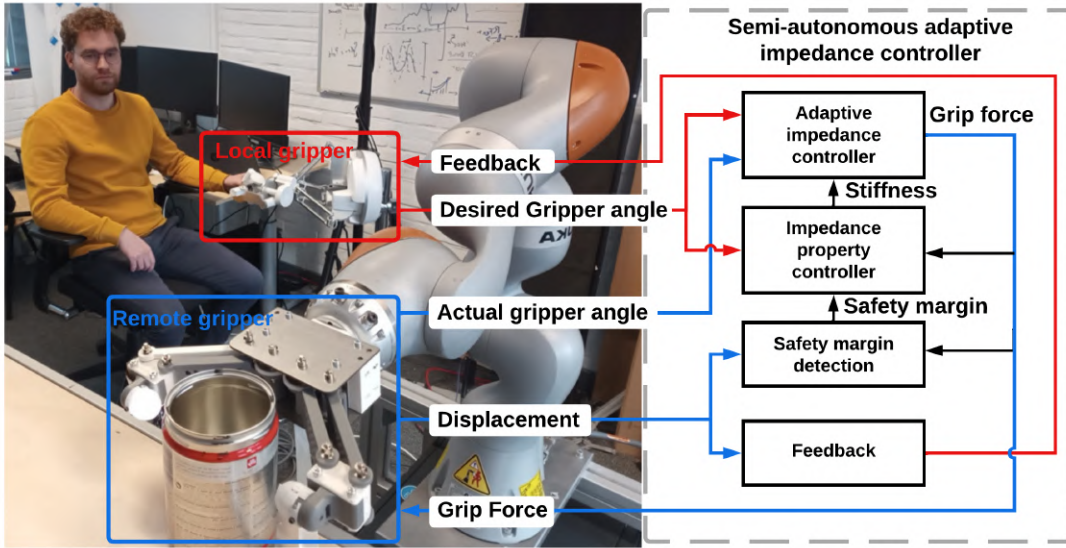


Fig. 3: Overview of the semi-autonomous adaptive impedance controller. On the left is a tele-grasping device. On the right is a schematic overview of the controller. The controller exists out of four parts: the adaptive impedance controller, the impedance property controller, the safety margin detection and feedback.

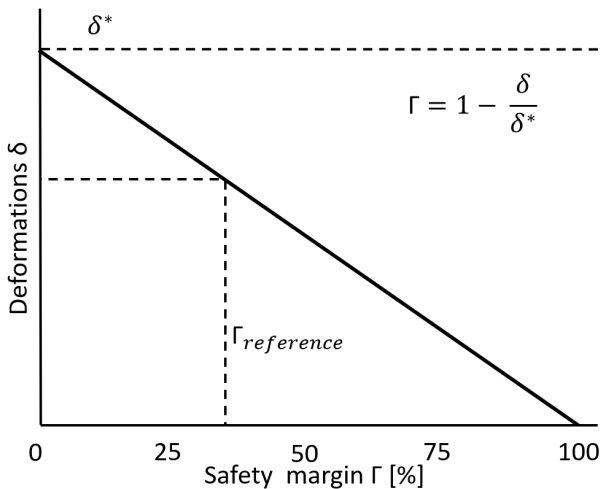


Fig. 4: The safety margin relative to the deformations in the contact area. The critical deformation ( $\delta^*$ ) at which gross slip occurs is represented by the horizontal line.

### 3.2 Adaptive impedance controller

The core of this method is an adaptive impedance controller. The controller computes a force which enables the gripper to move towards the desired gripper angle or apply a grip force. The adaptive impedance controller computes the force, as described in Equation 6.

$$F = K(\alpha_d - \alpha_a) + D(\dot{\alpha}_d - \dot{\alpha}_a) \quad (6)$$

With  $\alpha_d$ , the desired gripper angle demanded by the user,  $\alpha_a$  the actual gripper angle of the remote robot,  $K$  the stiffness term and  $D$  the damping value as the impedance properties.

### 3.3 Impedance property controller

The impedance property controller adapts the stiffness and damping term to a task. When the gripper is not grasping or touching an object, the stiffness term is set to a low value, the initial stiffness ( $K_0$ ), creating a low impedance controller. This low impedance controller achieves the desired position while being compliant with the environment to prevent unsafe situations, e.g. damaging objects.

When the gripper is in contact with an object, the stiffness term will become dependent on the safety margin to enable the adaptive impedance controller to apply a force equivalent to grasp stability. An Integrator controller adapts the stiffness based on the error between the reference safety margin and the detected safety margin.

$$K = K_0 + I \int e dt \quad (7)$$

$$e = \Gamma_r - \Gamma \quad (8)$$

With  $K_0$  the feedforward term of the controller which is equivalent to the initial stiffness,  $K$  the output stiffness term,  $I$  is the gain of the I controller,  $\Gamma$  the detected safety margin and  $\Gamma_r$  the reference safety margin.

To prevent delays in the system when there is a frequency difference between the safety margin detection and the desired gripper angle updates. The stiffness is computed based on the grip force, calculated with the last detected safety margin.

$$K = \frac{F_{gripper}}{x_d - x_a} \quad (9)$$

The damping term ( $D$ ) is always equal to the critical damping value to prevent undesired oscillations in the system, therefore, it scales with the stiffness term (Equation:10).

$$D = 2 \cdot 0.7\sqrt{K} \quad (10)$$

### 3.4 Feedback

Feedback informs the user that contact is present when the remote gripper touches an object. This feedback consists of a short vibration of 0.5s at the local gripper, activated during the initial moment of contact.

$$\theta_t = A \cdot \sin(2\pi \cdot f \cdot t) \quad (11)$$

With  $A$  the amplitude of the vibration,  $f$  the frequency of the vibration, and  $t$  the time.

To determine if the gripper has contact with an object, the contact area of the gripper is monitored. When deformations in the contact area exceed a threshold, there is contact with an object. Once the deformations exceed the threshold, the outside position of the object is stored ( $\alpha_{object}$ ). When the desired angle, demanded by the user, is greater than the angle of the grasped object,  $\alpha_d > \alpha_{object}$ , contact is lost.

## 4 EXPERIMENTS

We implemented the semi-autonomous impedance controller on a local-remote gripper setup to perform experiments (Section 4.1). Two experiments are conducted to test the controller's functionalities (Section 4.2). The first experiment, adaptability to external changes, evaluates if the controller (autonomously) maintains grasp stability during load force changes. The second experiment, adaptability to human input, test the user's control over the position of the remote gripper while holding an object.

### 4.1 Experimental setup

The local-remote gripper setup consists of a local haptic device (Sigma7) and a remote gripper (FUSE gripper). This gripper is mounted on a manipulator (KUKA iiwa7) to increase the degrees of freedom. The remote gripper has tactile sensors which act as the point of contact with the object to detect deformations for the safety margin (Section: 4.1.2). The deformations also indicate that the gripper is in contact with an object.



Fig. 5: Overview of the teleoperated gripper setup. The user controls the remote robot with the local haptic device, the SIGMA7. The remote robot exists out of a manipulator, the KUKA iiwa7, with at the end effector a gripper, the FUSE gripper. For tactile feedback, the remote gripper has tactile sensors, the ChromaTouch, on the gripper fingers.

### 4.1.1 Local-remote gripper

The user commands the desired position of the remote robot with the local gripper, the Sigma7 (Fig. 5). The Sigma7 has 7 degrees of freedom: 3 rotational, 3 translational and 1 gripper motion. For this research, the translational degrees of freedom of the sigma7 are limited to moving up and down (Heave). The rotational space is not restricted to provide the user comfort. However, the rotation of the local device is not an input for the pose of the remote gripper.

The remote robot consists of a FUSE gripper, which is mounted on a manipulator's end effector, the KUKA iiwa7. On this manipulator, an impedance controller adapts the pose. However, the rotation of the end effector is constant relative to the world frame to keep the remote gripper in a horizontal position. A scale factor ( $\theta$ ) translates the desired position demanded by the user to fit the range of motion of the remote manipulator.

$$\mathbf{F}_{endpoint} = \mathbf{K}(\mathbf{x}_d \cdot \theta - \mathbf{x}_a) + \mathbf{D}\left(\frac{d(\mathbf{x}_d \cdot \theta)}{dt} - \dot{\mathbf{x}}_a\right) \quad (12)$$

With  $\mathbf{F}_{endpoint}$ , the force at the end effector of the manipulator,  $\mathbf{K}$  the stiffness matrix,  $\mathbf{D}$  the damping matrix,  $\mathbf{x}_a$  and  $\mathbf{x}_d$  the actual position of the remote manipulator and the desired position demanded by the user, respectively.

The remote gripper, the FUSE gripper, is controlled with the proposed semi-autonomous adaptive impedance grip force controller, as described in the method. The FUSE gripper detects deformations in the contact area between the object and the gripper with tactile sensors (the ChromaTouch). The tactile sensors form the point of contact between the object and the gripper. More details about deformation detection are in Section 4.1.2. As the FUSE gripper is used as a tool, we do not discuss the details of this gripper. More information on the gripper is in Appendix A.

### 4.1.2 Deformation tracking in the contact area

The tactile sensor on the FUSE gripper is the ChromaTouch. This sensor has a deformable dome in which two layers of coloured dots are present, which are captured by a camera, as shown in Fig. 6. When the sensor is indented or a shear force is applied, the position, shape and colour of the dots change. Deformations in the contact area are captured by tracking the changes in shape and position of the dots. We neglect the colour changes of the dots in this research as these are not of value during deformation detection.

The deformation is computed by tracking the position of the dots in the dome using OpenCV computer vision software (Fig. 7). In every image, 20 dots in the centre of the image are detected and labelled with the nearest neighbour algorithm. The labelled dots correspond to the same dot in the previous frame. Comparing the vertical position of the dots in different images gives the deformation. To reduce the noise in the position data caused by OpenCV, the average displacement of the 20 dots is placed into a moving time window of 10. The output of this window is the deformation ( $\delta$ ) in the contact area. More information about the sensor and the dot detection method is provided in Appendix B.

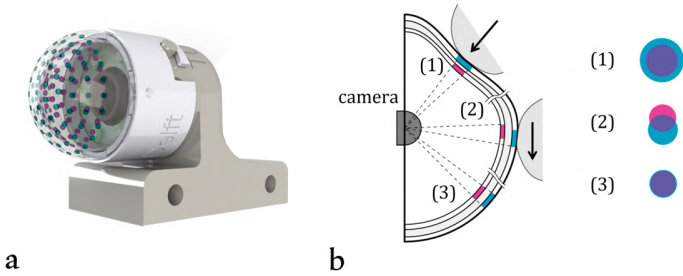


Fig. 6: a) The ChromaTouch sensor. b) The two-layered dotted dome of the sensor, 1) deformations caused by indentation, 2) deformations caused by shear force, 3) the dome during steady-state. [30]

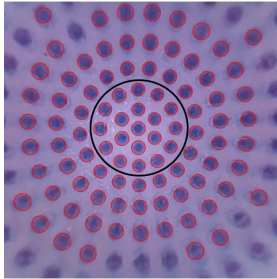


Fig. 7: Image of the inside of the ChromaTouch. The red circles are the detected dots with computer vision. The dots encircled by the black line are the 20 center dots tracked for the deformation.

## 4.2 Experimental protocol

A participant performed two experiments with the semi-autonomous adaptive impedance controller to test the controller's functionalities. The first experiment, adaptability to external changes, evaluate if the controller maintains grasp stability during load force changes. To maintain grasp stability, the controller has to stabilize the safety margin around the reference margin. To do this, we expect the controller to adapt the stiffness term to change the grip force according to the load force.

The second experiment, adaptability to human input, tests the user's control over the position of the remote gripper while holding an object. While the participant holds the object with the remote gripper, he perturbs the input angle. We expect that these input perturbations cause the controller to adapt the stiffness term to maintain the reference safety margin when the perturbations are inside the object. If the commanded angle becomes larger than the object, the gripper should open.

For comparison, we performed both experiments once with a force or low-impedance controller. These controllers are chosen as they are both commonly used. We use a low impedance controller (stiffness = 60 N/m) as a baseline for the first experiment, adaptability to external changes. A force controller was not selected as it can not adapt its grip force to external perturbations. For the second experiment, adaptability to human input, a force controller (2N) is used as a baseline. We did not implement the low-impedance controller, as the force applied by this controller directly depends on the desired gripper angle (Equation: 6). As this

research is a proof of concept, one participant performs all the experiments.

### 4.2.1 Settings

The participant performs the experiments while maintaining visual contact with the remote gripper by sitting in front of the remote device. The local device is positioned between the participant and the remote manipulator, which the participant controls with his right hand. Within the remote robot's range of motion, a flat surface is present to grasp and lift objects from (Fig. 5).

During the experiments, all parameters are set to the following values (Table 1).

Defenition	Symbol	Value
Feed forward value (initial stiffness)	$K_0$	20 [N/m]
Stiffness manipulator	$\mathbf{K}$	20 [N/m]
I gain	$I$	5
Reference grip force safety margin	$\Gamma_d$	30
Force conversion factor	$\eta$	0.018
Scale factor	$\theta$	10
Minimal grip force	$F_{min}$	0.6 [N]
Amplitude of feedback	$A$	1
Frequency of feedback	$f$	4 [Hz]

TABLE 1: Parameters for the experiments

### 4.2.2 Critical deformation

Before conducting the experiments using the semi-autonomous adaptive impedance controller, we need to gather critical deformation data. This data is used to calculate the safety margin, as described in Equation 4. The critical deformation ( $\delta^*$ ) is object and grip force dependent. Therefore a dataset of critical deformations must be collected for a range of grip forces.

To detect the critical deformation data set, the following protocol is used:

- 1) Grasp an object with the remote gripper, with a constant grip force.
- 2) Lift and hold the object in midair.
- 3) Add weight to the object until it shows displacement, gross slippage.
- 4) Analyze the deformation data of the contact surface, and note the deformation measured at the verge of slippage, this is the critical deformation.
- 5) Repeat this sequence for multiple grip forces and define a relation between the applied grip force and deformations.

For our experiments, the critical deformation is collected for seven different grip forces between 0 and 1.5 N. For more details about the critical deformation, see Appendix C.

### 4.2.3 Experiment 1: Adaptability to external changes

To test the adaptability to external changes, a participant operates the tele-grasping device and performs a pick-and-place task with a metal can. While the object is held in mid-air, extra load force is added. The participant takes the following steps:

- 1) **Close:** The participant closes the remote gripper to grasp the object.
- 2) **Lift and hold:** The participant lifts the object with the remote gripper from the surface it was standing and holds it in midair.

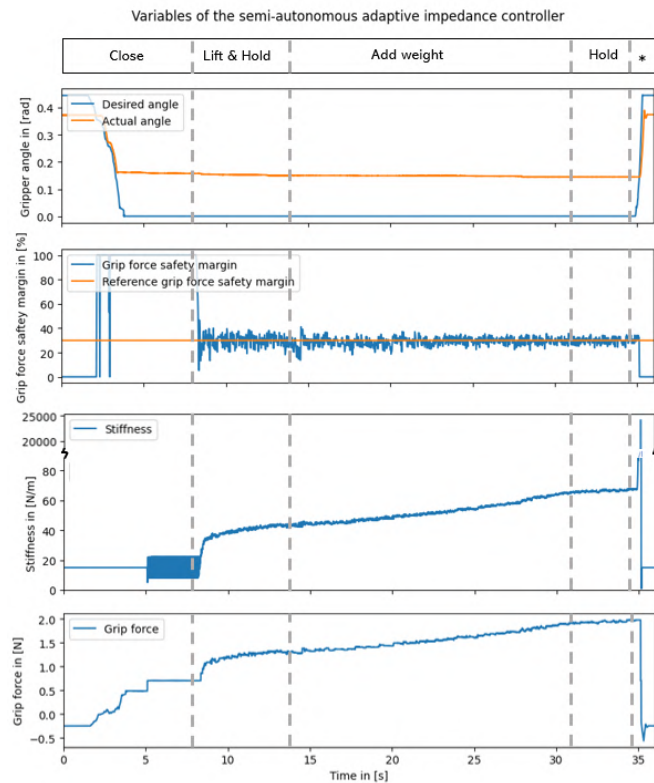


Fig. 8: Adaptability to external changes: results of the semi-autonomous adaptive impedance grip force controller. \* is place and open

- 3) **Add weight:** A non-participant continuously adds weight (100 gr of rice) to the object while the user holds the object in midair.
- 4) **Hold:** After the weight addition, the participant holds the object in midair.
- 5) **Place and Open:** At last, the participant places the object with the additional weight on the surface and opens the gripper.

#### 4.2.4 Experiment 2: Adaptability to human input

During the second experiment, the participant holds an object, the metal can, in midair with the teleoperated gripper device. While the object is held, the user perturbs the reference angle with an increasing magnitude until the gripper opens. The participant follows this protocol:

- 1) **Hold object:** The participant holds the object in midair.
- 2) **Gripper angle perturbation:** The participant perturbs the desired gripper angle. The perturbations start small but increase in size over time.
- 3) **Gripper open:** The experiment stops when the gripper opens.

## 5 RESULTS

Four experiments have been performed, two to evaluate the functionalities of the proposed semi-autonomous controller and two supplementary for comparing our approach to either a force controller or constant low-impedance controller. During all experiments, we obtained four plots: the desired and actual gripper angle of the local-remote device, the

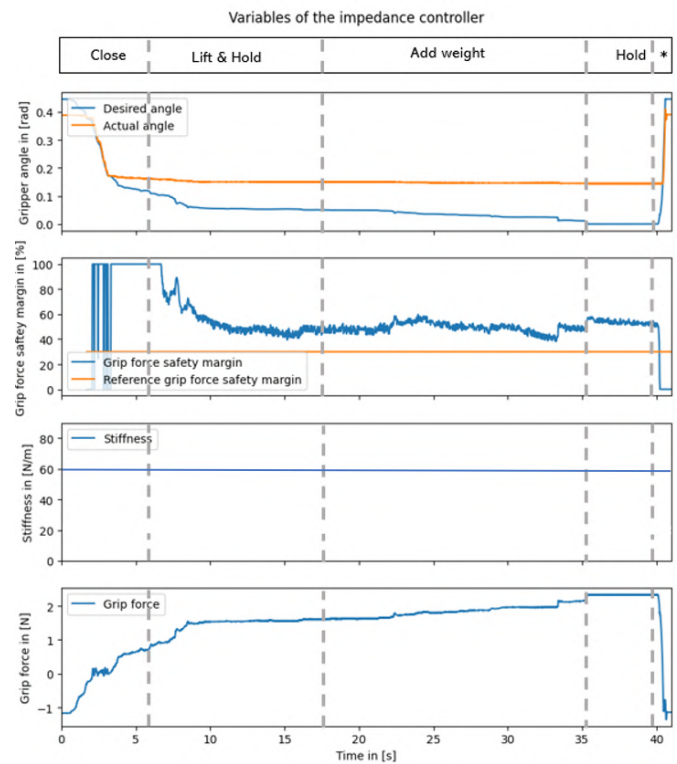


Fig. 9: Adaptability to external changes: results of the low-impedance controller. \* is place and open

safety margin to analyse grasp stability, the stiffness term of the (adaptive) impedance controller and the grip force at the remote gripper. In this section, we first discuss the results of the controller's adaptability to external perturbations and, secondly, the adaptability to human input.

### 5.1 Adaptability to external changes

Here we present the results of the proposed semi-autonomous adaptive impedance controller during external changes and the supplementary results of a low-impedance controller.

#### 5.1.1 Semi-autonomous adaptive impedance controller

Fig. 8 shows the results of the proposed semi-autonomous adaptive impedance controller. In the first row of the graph, we can see that the user opened and closed the remote gripper. However, the actual angle of the remote gripper stops following the desired angle once the object is grasped. This is clearly visible by the constant difference between the desired and actual gripper angle. When the desired gripper angle becomes larger than the actual gripper angle of the remote robot, the desired angle is followed again.

The second row illustrates the safety margin. The safety margin is 0 when the gripper does not touch the object. Once the gripper closes and establishes contact, the safety margin is 100% as there is no load force present (the object is still standing on the table). As the gripper lifts and holds the object, the controller upholds a safety margin similar to the

reference safety margin of 30 %. The reference safety margin represents grasp stability. Furthermore, the controller maintains the desired safety margin when the load force increases.

On the safety margin data noise is present. One possible source could be the precision of the dot detection method, which is used as an input to compute the deformation and, thus the safety margin. However, the noise does not influence the research and is thus not investigated further.

To sustain a safety margin of 30%, the semi-autonomous adaptive impedance controller adjusts its stiffness while the load force increases, as shown in the third column of the figure. The stiffness term increases to adapt the grip force to the load force during the lifting phase of the object and the weight addition. The resulting grip force is illustrated in the last row. An extreme stiffness fluctuation to maintain the desired safety margin is at  $t = 35.5$  s. The stiffness term peaks before the desired angle surpasses the actual gripper angle to open the remote gripper. To maintain the 30% safety margin and thus the corresponding grip force, the stiffness increases to counteract the small difference between the desired and actual gripper angle.

Another particular behaviour in the stiffness term occurs during  $t = 5$  s and  $t = 8$  s, as the stiffness fluctuates around 15 N/m. These fluctuations are present because the autonomous impedance property controller tries to reduce the grip force as the safety margin is higher than desired. To reduce the grip force, the controller decreases the stiffness term. However, this is ineffective as the computed force is lower than the minimum required force. As a result, the minimal grip force is applied instead (Equation: 5). This fluctuation in the stiffness term does not cause undesired behaviour in the grip force and therefore does not influence the outcome of this experiment.

The results of this experiment show that the semi-autonomous controller maintains grasp stability during external perturbations. At the same time, the user controls the position of the remote gripper, and the grip force is controlled autonomously.

### 5.1.2 Low-impedance controller

Fig. 9 shows the results of the low-impedance controller, which we used as a comparison. The first row of the figure shows that the remote gripper follows the desired gripper angle commanded by the user while closing. When the remote gripper touches the object, the gripper stops following the commanded angle. While the difference in gripper angle increases and the stiffness remains constant, the grip force grows, as depicted in the last two rows.

When weight is added to the object, the participant enlarges the difference between the desired and actual gripper angle to increase the grip force. However, in the second row, we can see that the safety margin is higher than the reference safety margin while the participant lifts and holds the object. This indicates that the grip force is higher than needed for a stable grasp.

While observing the second row, the safety margin fluctuates between 0 and 1 at  $t = 2.5$  s. These fluctuations do not result in undesired behaviour and are explainable. A small grip force is applied when the gripper makes contact with the object. The grip force causes little to no deformation in

the contact surface as there is no load force and therefore corresponds with a safety margin of 1. However, a small grip force corresponds with a small critical deformation, but the measured deformations are sometimes larger. When the detected displacement in the contact surface exceeds the critical displacement, it causes the safety margin to drop to 0.

The results show that the low-impedance controller cannot autonomously adapt to external load force changes. But, the user can modify the grip force by adapting the difference between the local and remote gripper angles. However, this does not guarantee the desired safety margin, compromising grasp stability.

## 5.2 Experiment 2: Adaptability to human input

In this section, we present the results of the proposed semi-autonomous adaptive impedance controller's adaptability to human input, and the supplementary results of the force controller.

### 5.2.1 Semi-autonomous adaptive impedance controller

Fig. 10 displays the variables of the proposed semi-autonomous adaptive impedance controller during the adaptability to human input experiment. In the first row of the figure, we can see the participant perturbing the desired gripper angle while holding an object with the remote gripper. As the desired angle is smaller than the actual angle, the remote gripper does not change position due to the object it is holding. When the desired angle becomes larger than the one of the remote, the remote gripper follows the desired angle and opens.

As seen in the second row of the figure, the safety margin maintains the desired 30% while the remote gripper holds the object. When the gripper opens, the safety margin drops to 0 as no object is held anymore.

The last two rows display the stiffness term and grip force, respectively. While the participant holds the object, a constant grip force is applied to maintain the 30% safety margin as no load force changes occur. To maintain the grip force, the stiffness term adjusts to compensate for the changing difference between the desired and actual gripper angle. As the difference in gripper angle becomes smaller, the stiffness term increases to maintain the constant grip force, as can be seen at  $t = 4$  s,  $t = 6$  s and  $t = 8$  s.

These results show that the controller can adapt to human input to maintain grasp stability. Grasp stability is achieved by adapting the stiffness term autonomously to regulate the grip force while the user maintains the ability to open the gripper.

### 5.2.2 Force controller

Fig. 11 illustrates the results of the force controller, which we used as a comparison. As we can see in the last row of the figure, the controller applies a constant grip force of 2 N at the remote gripper. However, the applied grip force is not equivalent to grasp stability. The second row in the figure shows us that the margin is higher than the desired 30%.

In addition, the force controller does not adapt to the positional commands of the participant as it only applies a force. Therefore, the desired angle is not used as an input

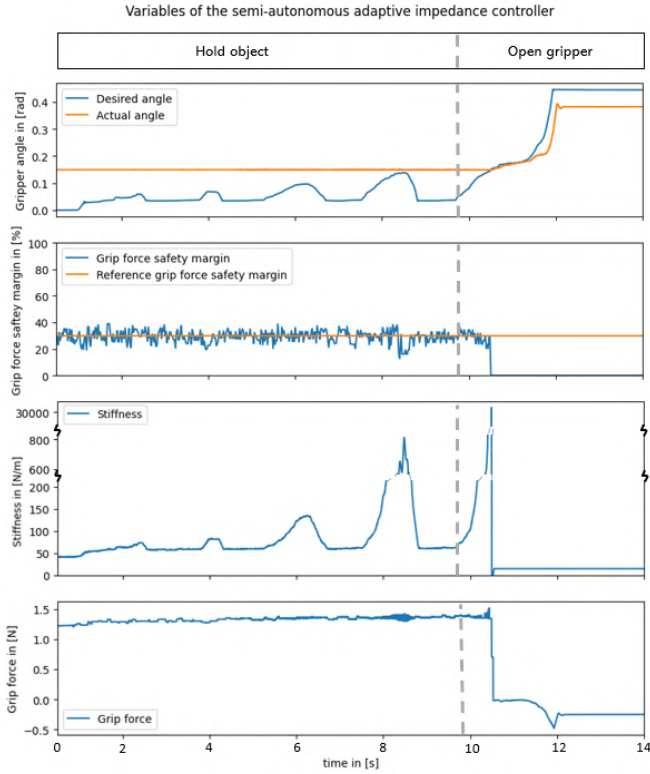


Fig. 10: Adaptability to human input: results of the semi-autonomous adaptive impedance grip force controller

as seen in the figure’s first row. This makes it impossible for the participant to open or close the gripper with their commands.

These results indicate that the force controller does not adapt to human input and cannot adjust the opening and closing of the gripper according to the desired angle by the user. The controller lacks the ability to adjust the grip force to achieve grasp stability.

### 5.3 Overview

We conducted and analyzed multiple experiments and controllers. A brief overview of the controllers and their performance is captured in Table 2.

The proposed semi-autonomous controller proved itself to adapt autonomously to external changes and human input. In contrast, the force controller cannot adapt to human input or external changes. No experiments were performed to evaluate the force controller’s response to external changes as it was conceptually inadequate. The low-impedance controller is also not able to adapt autonomously to external changes. However, the user can adapt their input to the grip force. As the user directly controls the grip force based on the difference in desired and actual gripper angle, the low-impedance controller cannot maintain grasp stability during human input perturbations.

## 6 DISCUSSION

The purpose of this study was to develop a teleoperated control method which regulates the grip force au-

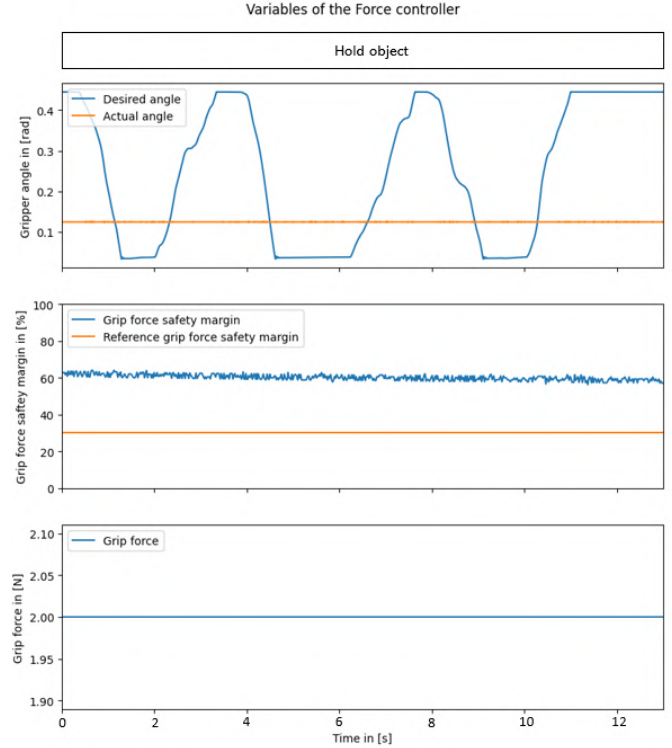


Fig. 11: Adaptability to human input: results of the force controller. The stiffness term is not present in this figure, as a force controller does not have this variable.

Functionalities	Controllers	semi-auto*	Force	Low-impedance
Adaptive to external changes		yes	No**	Yes
Adaptive to human input		yes	No	No**

TABLE 2: An overview of the tested controllers and their capability. \* Semi-autonomous adaptive impedance controller. \*\* Note: No experiments are performed to test this functionality because the controller’s response is conceptually inadequate.

tonomously to maintain grasp stability while the user remains in control of the position of the remote gripper. To achieve this goal, we introduced a semi-autonomous adaptive impedance controller. We evaluated the semi-autonomous controller’s functionalities by testing its adaptability to external changes and human input.

The results of the experiments show that the semi-autonomous controller maintains grasp stability during load force changes and human input perturbations. The experiments also validate that the design objectives have been met, as the grip force is controlled autonomously while the user maintains control over the gripper angle. To prove that the semi-autonomous controller is an improvement over force, low-impedance, and adaptive impedance control, we will compare the supplementary results of the experiments that involve the force and low-impedance controllers with those of the semi-autonomous controller. In addition, we compared the semi-autonomous controller and state-of-the-art adaptive impedance methods to highlight their differences.

While both the low-impedance and force controllers do

not fit the design goal of this research, this does not have to influence their functionalities to be adaptive to external changes and human input. The low-impedance cannot control the grip force autonomously, the force depends on the difference in desired and actual gripper position. However, this enables the low-impedance controller to maintain control over the position of the remote gripper. Although the low-impedance controller only meets one of the two design objectives, it can adapt to external changes, similar to the semi-autonomous controller. As the user controls the desired position, the user can adapt the grip force at the remote gripper to external changes, such as load force changes, as shown in Fig. 8. However, the applied force does not guarantee grasp stability.

The tele-grasping setup has no feedback, which makes the user unaware if the grip force is close to grasp stability. While implementing feedback could provide information about grasp stability, it would not make the low-impedance controller equivalent to the semi-autonomous controller, as the low-impedance controller cannot adapt to human input perturbations. The desired gripper angle is directly translated into a grip force, which causes grip force perturbations. This disables the user to apply a constant grip force while the input is perturbed. The force controller does not fit any of the design objectives. The user can not control the gripper's position, or adapt the grip force at the remote robot, see Fig 11. As the grip force is constant, it also cannot adapt to external perturbations, which limits the controller's functionalities. However, this does help in being resilient to human input changes as there is no input. The force and low-impedance controller cannot replicate all the functionalities of the semi-autonomous controller.

The functionalities of the designed semi-autonomous adaptive impedance controller stand out from low-impedance and force controllers. However, it is not the first (semi-autonomous) adaptive impedance controller. Compared to other state-of-the-art adaptive impedance controllers [28], [31], [32], our method has a unique focus on grasping. While other controllers use adaptive impedance control to adjust the forces at the endpoint of a manipulator, our implementation focuses on the forces at the remote gripper. The proposed semi-autonomous controller prevents slippage and an extensive amount of force by proactively regulating the grip force instead of a manual response of the user to slipping or damage that has already occurred to the object. Nevertheless, autonomously managing the grip force with an adaptive impedance controller has been done before by Brygo et al. Their controller also enables the user to control the position of the remote gripper while the force is controlled independently. However, their method does not specifically adapt the grip force in the gripper and instead adjusts the stiffness of all joints based on load force changes, which might be unnecessary. This method is also unable to detect slippage and adapt correspondingly to maintain grasp stability. But, adapting the applied force based on the load force makes this method applicable to all objects. This is possible because the load force can be measured with any sensor without prior knowledge, making it suitable for use in a diverse environment. However, if the load-to-grip force relation is incorrect, the grip force might cause slippage or damage to the object as grasp stability is not guaranteed.

Our controller requires the critical displacement, a known variable, to achieve grasp stability. Since the critical displacement is object dependent, we must detect what object is being grasped to apply the appropriate critical displacement dataset. Nevertheless, the semi-autonomous adaptive impedance controller guarantees grasp stability during external perturbations and human input changes. The controller proves itself to be proactive to object slippage. Therefore we are convinced that the designed semi-autonomous adaptive impedance controller brings tele-grasping one step closer to human-like grasping.

As the semi-autonomous controller relies on the safety margin to maintain grasp stability, we recommend further research on object-independent safety margin detection to reduce the dependency on the critical deformation. Already promising research is done with machine learning to compute the safety margin without prior known object properties [29]. However, a significant disadvantage of this approach is the need for a large amount of training data. Therefore, we recommend continuing research into alternative safety margin detection methods to grasp an unknown object. Another limitation while detecting the safety margin occurs while detecting the deformations in the contact area with the ChromaTouch sensor. As the sensor dome is stiff, displacement of the dots only occur when there is a pre-applied force. When handling delicate objects, this is undesired. Therefore, we strongly recommend more flexible domes to make them usable for small forces ( $< 0.5$  N).

## 7 CONCLUSIONS

This research started with a design objective to develop a semi-autonomous controller for teleoperated object grasping where the user controls the position of the remote gripper, and the remote robot controls the grip force to maintain grasp stability. To achieve these objectives we successfully implemented a semi-autonomous adaptive impedance grip force controller. The semi-autonomous controller facilitates the autonomous control of the grip force to maintain grasp stability, achieved by adapting the stiffnesses term based on the safety margin. Meanwhile, the user is in control of the gripper angle.

The designed controller prevents slippage by applying a stable grasp. From now on, the user can remotely grasp objects confidently as grasp stability is maintained during external changes and human input perturbations. This is a significant improvement compared to the low-impedance and force controller, which do not maintain a stable grasp.

Overall, we conclude that teleoperated grasping with the semi-autonomous adaptive impedance controller is successful. The user no longer needs to worry about controlling the grip force, freeing up their focus to complete their task, whether it is a rescue mission, space operation, or remote surgery. The user can now concentrate on their expertise without worrying about slip.

## ACKNOWLEDGEMENTS

I would like to thank Dr. Luka Peternel and Dr. Michaël Wiertelwsk for their support and guidance during this project. A big thank you to Dr. Laurence Willemet and Dirk

Jan Boonstra for all their help with the ChromaTouch sensor and the co-operation while building the grippers. I also want to show my appreciation to Dr. Micah Prendergast for helping out with the KUKA and Sigma7.

## REFERENCES

- [1] M. J. Schuster, M. G. Müller, S. G. Brunner, *et al.*, “The arches space-analogue demonstration mission: Towards heterogeneous teams of autonomous robots for collaborative scientific sampling in planetary exploration,” *IEEE Robotics and Automation Letters*, vol. 5, no. 4, pp. 5315–5322, 2020.
- [2] B. M. Moghaddam and R. Chhabra, “On the guidance, navigation and control of in-orbit space robotic missions: A survey and prospective vision,” *Acta Astronautica*, vol. 184, pp. 70–100, 2021.
- [3] S. S. Alam, T. Ahmed, M. S. Islam, and M. M. F. Chowdhury, “A smart approach for human rescue and environment monitoring autonomous robot,” *International Journal of Mechanical Engineering and Robotics Research*, vol. 10, no. 4, pp. 209–215, 2021.
- [4] C. Cruz Ulloa, G. Prieto Sánchez, A. Barrientos, and J. Del Cerro, “Autonomous thermal vision robotic system for victims recognition in search and rescue missions,” *Sensors*, vol. 21, no. 21, p. 7346, 2021.
- [5] M. Bernard, K. Kondak, I. Maza, and A. Ollero, “Autonomous transportation and deployment with aerial robots for search and rescue missions,” *Journal of Field Robotics*, vol. 28, no. 6, pp. 914–931, 2011.
- [6] C. Preusche, T. Ortmaier, and G. Hirzinger, “Teleoperation concepts in minimal invasive surgery,” *Control engineering practice*, vol. 10, no. 11, pp. 1245–1250, 2002.
- [7] I. El Rassi and J.-M. El Rassi, “A review of haptic feedback in tele-operated robotic surgery,” *Journal of medical engineering & technology*, vol. 44, no. 5, pp. 247–254, 2020.
- [8] M. Shahbazi, S. F. Atashzar, and R. V. Patel, “A systematic review of multilateral teleoperation systems,” *IEEE transactions on haptics*, vol. 11, no. 3, pp. 338–356, 2018.
- [9] R. S. Johansson and J. R. Flanagan, “Coding and use of tactile signals from the fingertips in object manipulation tasks,” *Nature Reviews Neuroscience*, vol. 10, no. 5, pp. 345–359, 2009.
- [10] R. S. Johansson and G. Westling, “Roles of glabrous skin receptors and sensorimotor memory in automatic control of precision grip when lifting rougher or more slippery objects,” *Experimental brain research*, vol. 56, no. 3, pp. 550–564, 1984.
- [11] M. Santello, M. Flanders, and J. F. Soechting, “Patterns of hand motion during grasping and the influence of sensory guidance,” *Journal of Neuroscience*, vol. 22, no. 4, pp. 1426–1435, 2002.
- [12] R. S. Johansson and K. J. Cole, “Sensory-motor coordination during grasping and manipulative actions,” *Current opinion in neurobiology*, vol. 2, no. 6, pp. 815–823, 1992.
- [13] D. Kruse, J. T. Wen, and R. J. Radke, “A sensor-based dual-arm tele-robotic system,” *IEEE Transactions on Automation Science and Engineering*, vol. 12, no. 1, pp. 4–18, 2014.
- [14] B. L. Luk, K. Liu, A. A. Collie, D. S. Cooke, and S. Chen, “Tele-operated climbing and mobile service robots for remote inspection and maintenance in nuclear industry,” *Industrial Robot: An International Journal*, 2006.
- [15] C. Yang, G. Peng, L. Cheng, J. Na, and Z. Li, “Force sensorless admittance control for teleoperation of uncertain robot manipulator using neural networks,” *IEEE Transactions on Systems, Man, and Cybernetics: Systems*, vol. 51, no. 5, pp. 3282–3292, 2019.
- [16] A. Ajoudani, S. B. Godfrey, M. Bianchi, *et al.*, “Exploring teleimpedance and tactile feedback for intuitive control of the pisa/iit soft hand,” *IEEE transactions on haptics*, vol. 7, no. 2, pp. 203–215, 2014.
- [17] G. A. Christiansson and F. C. Van Der Helm, “The low-stiffness teleoperator slave—a trade-off between stability and performance,” *The International journal of robotics research*, vol. 26, no. 3, pp. 287–299, 2007.
- [18] A. Ajoudani, C. Fang, N. G. Tsagarakis, and A. Bicchi, “A reduced-complexity description of arm endpoint stiffness with applications to teleimpedance control,” in *2015 IEEE/RSJ international conference on intelligent robots and systems (IROS)*, IEEE, 2015, pp. 1017–1023.
- [19] Y. Michel, R. Rahal, C. Pacchierotti, P. R. Giordano, and D. Lee, “Bilateral teleoperation with adaptive impedance control for contact tasks,” *IEEE Robotics and Automation Letters*, vol. 6, no. 3, pp. 5429–5436, 2021.
- [20] S. H. Tabatabaei, A. H. Zaeri, and M. Vahedi, “Design an impedance control strategy for a teleoperation system to perform drilling process during spinal surgery,” *Transactions of the Institute of Measurement and Control*, vol. 41, no. 10, pp. 2947–2956, 2019.
- [21] S. Klevering, W. Mugge, D. A. Abbink, and L. Peternel, “Foot-operated tele-impedance interface for robot manipulation tasks in interaction with unpredictable environments,” in *2022 IEEE/RSJ International Conference on Intelligent Robots and Systems (IROS)*, IEEE, 2022, pp. 3497–3504.
- [22] A. Scibilia, M. Laghi, E. De Momi, L. Peternel, and A. Ajoudani, “A self-adaptive robot control framework for improved tracking and interaction performances in low-stiffness teleoperation,” in *2018 IEEE-RAS 18th International Conference on Humanoid Robots (Humanoids)*, 2018, pp. 280–283. DOI: 10.1109/HUMANOIDS.2018.8625062.
- [23] L. Peternel, T. Petrič, and J. Babič, “Robotic assembly solution by human-in-the-loop teaching method based on real-time stiffness modulation,” *Autonomous Robots*, vol. 42, no. 1, pp. 1–17, 2018.
- [24] L. Peternel, N. Beckers, and D. A. Abbink, “Independently commanding size, shape and orientation of robot endpoint stiffness in tele-impedance by virtual ellipsoid interface,” in *2021 20th International Conference on Advanced Robotics (ICAR)*, IEEE, 2021, pp. 99–106.

- [25] D. S. Walker, R. P. Wilson, and G. Niemeyer, "User-controlled variable impedance teleoperation," in *2010 IEEE International Conference on Robotics and Automation*, IEEE, 2010, pp. 5352–5357.
- [26] E. Hocaoglu and V. Patoglu, "Semg-based natural control interface for a variable stiffness transradial hand prosthesis," *Frontiers in Neurorobotics*, vol. 16, 2022.
- [27] A. Ajoudani, N. Tsagarakis, and A. Bicchi, "Tele-impedance: Teleoperation with impedance regulation using a body-machine interface," *The International Journal of Robotics Research*, vol. 31, no. 13, pp. 1642–1656, 2012.
- [28] A. Brygo, I. Sarakoglou, N. Tsagarakis, and D. G. Caldwell, "Tele-manipulation with a humanoid robot under autonomous joint impedance regulation and vibrotactile balancing feedback," in *2014 IEEE-RAS International Conference on Humanoid Robots*, IEEE, 2014, pp. 862–867.
- [29] D. Boonstra, "Learning to estimate the proximity of slip using high-resolution tactile sensing," *Master Thesis*, 2022.
- [30] C. Langens, "Controlling grip force by maintaining a constant frictional safety margin to improve robotic grasping," *Master Thesis*, 2022.
- [31] Y.-C. Huang, D. A. Abbink, and L. Peternel, "A semi-autonomous tele-impedance method based on vision and voice interfaces," in *2021 20th International Conference on Advanced Robotics (ICAR)*, IEEE, 2021, pp. 180–186.
- [32] L. Muratore, A. Laurenzi, E. M. Hoffman, *et al.*, "Enhanced tele-interaction in unknown environments using semi-autonomous motion and impedance regulation principles," in *2018 IEEE International Conference on Robotics and Automation (ICRA)*, IEEE, 2018, pp. 5813–5820.

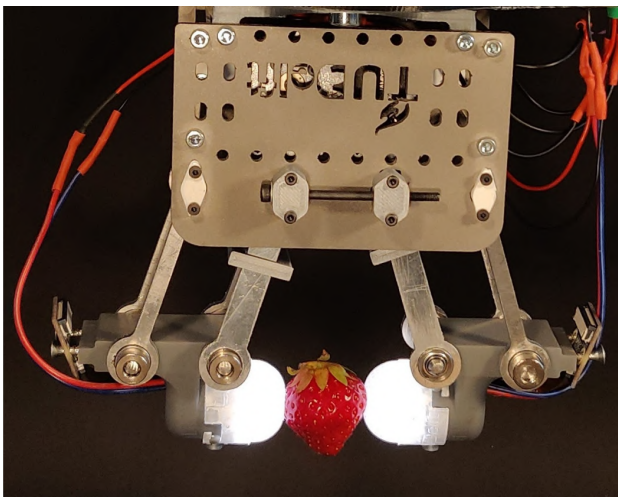
## APPENDIX A

### THE FUSE GRIPPER

The FUSE gripper is designed to grasp delicate objects with small forces. The gripper has tactile sensors at the end effectors to provide information about the contact surface between the grasped object and the gripper. For this project, we made the second iteration of this gripper. This appendix will discuss the technical specification and improvements compared to the first iteration, a build manual and the force conversion factor to compute the end-effector force in Newton.

#### Technical specifications

The design of the FUSE gripper is based on the two tactile sensors at the end effectors. These sensors, the ChromaTouch, require a constant point of contact. Therefore, the gripper fingers are connected to the gripper body with a four-bar mechanism (Fig. 1). An angular power transmission drives the four-bar mechanism to maintain symmetry in the applied forces at the end effector of the gripper. The power transmission exists out of a servo motor and three gears with a 1:1 ratio. To minimise friction in the system, the rotational parts are mounted on the gripper body with bearings. More details about the ChromaTouch sensor are in Appendix B.



(a) 1st generation (Tactile Machines Lab, “Demo fuse gripper v1,” 2022, Delft University of Technology)



(b) 2nd generation

Fig. 1: The FUSE gripper

#### Improvements

The design of the second iteration has multiple improvements in wear, manufacturability and assembly compared to the first gripper. To reduce wear and backlash POM gears are implemented instead of aluminium laser-cut gears.

Regarding manufacturability and assembly, the number of parts is reduced for the four-bar mechanism by 3D printing the gripper fingers instead of laser-cutting. 3D printing also improved the assembly and cable management. The design now features cable trays for organized cable management and the sensor is made modular. The modular design allows easy removal of the tactile sensors. A dedicated box maintains the four-bar mechanism and provides a secure mount for the sensors, eliminating the need for complete reassembly in case of sensor replacement.

#### Other investigated improvements (not implemented)

Before implementing the previously discussed improvements, the design of the FUSE gripper was reviewed. Multiple ideas were discussed but not implemented. To ensure these ideas are remembered, we will include them here.

Instead of implementing an angular gripper, a linear gripper was considered. However, this idea was not further exploited as a linear gripper shows more friction in its system. Another possibility was to adapt the angular power transmission from gears to a belt drive. A belt drive should have less backlash and friction and requires less precision during the assembly of the transmission. However, due to time restrictions, the belt drive was not researched further as it changes the design of the gripper significantly.

## Build manual

The gripper consists of standardised components, with three exceptions: the 3D resin-printed gripper fingers, the laser-cut gripper body and the custom POM gears.



Fig. 2: 3D render of the 2nd iteration FUSE gripper

### Part list

- 1x Dynamixel XH430-W210-R
- 1x Dynamixel U2D2
- 1x SMPS2Dynamixel
- 1x Powersupply 12V
- 2x Bearings 4mm I.D., 8mm O.D.
- 16x Bearings 4mm I.D., 10mm O.D.
- 16x Modelcraft adjustable rings (4mmx8mmx5mm)
- 4x brass Hex threaded standoff, female/female 50mm M4
- stainless steel 3mm
- stainless steel rod 4mm
- 1x Emergency stop button
- 3x POM Gears 70T 0.5M
- 2x ChromaTouch tactile sensor

### Custom parts

- 2x gripper fingers, IWM, 3D resin print
- 2x ChromaTouch, Tactile machines lab
- 3x POM gears 70T 0.5, adapted by the IWM
- 2x Sensor box, IWM, 3D print
- 3x Gear mount plates, IWS, laser-cutting
- 2x Gripper body plates, IWS, laser-cutting

To build the gripper first manufacture the custom parts, above is a list with the parts, and where they could be produced. When all parts are present start with glueing the bearings into the gripper fingers. Next, mount the gears to the gripper fingers and the motor. The motor has to be screwed to one of the gripper body plates to ensure it does not move. To align the gears, the steel rods must be inserted in the gripper fingers and between the gripper plates. This has to be perfect. Otherwise, there will be losses in the power transmission. The rods are kept in place by adjustable rings outside

the gripper body. As last, the ChromaTouch sensor and its designated box are mounted at the fingertips, establishing the four-bar mechanism. For a clear overview see Fig.2 For a more in depth description of the build process of the fuse gripper, see [https://docs.google.com/document/d/1RBDI7jy-PIYnK\\_j0WH-F8FypHqbOF13j6fQi\\_Sp\\_P54/](https://docs.google.com/document/d/1RBDI7jy-PIYnK_j0WH-F8FypHqbOF13j6fQi_Sp_P54/)

The system’s wiring includes an emergency button for safety. An overview of the wiring is illustrated in Fig. 3

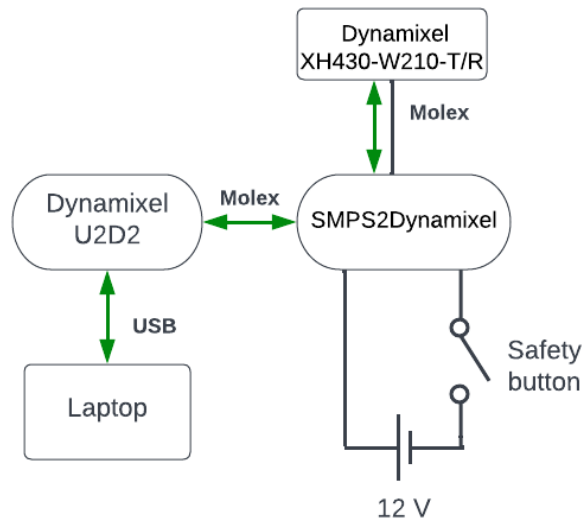


Fig. 3: The wiring of the FUSE gripper. The black lines are the electrical wires. The green arrows show the data connections.

**Current-force conversion factor**

A current-force conversion factor is calibrated to know the force applied by the gripper at its end effectors. Different force measurements at different currents are collected. The average force applied per current is used as a dataset to fit a linear line. The growth factor of this linear line is the force conversion factor

For the force measurements, we use the ATI Nano 43 FT Force sensor. The Force sensor is placed between the tactile sensors at the end effector of the gripper. The sensor is in midair while the gripper grasps it with the commanded current. Holding the sensor in midair reduces the forces caused by friction. If the sensor was standing on a table, friction between the table and the sensor could cause inaccurate measurements. Data with different current intervals are collected between 0 and 269 mA to take the static friction of the system into account. The intervals for data collection are equal to 2.69, 5.38, 13.45 and 26.9 mA.

**Results**

The current-force conversion factor, is 0.016. This number is the average linear factor between the four different current intervals (Table: 1). The raw data during the force measurements can be seen in Fig. 4.

Interval in (mA)	Linear fit (a)
2.69	0.01587
5.38	0.01464
13.45	0.01581
26.90	0.01981

TABLE 1: A linear line,  $ax + b$  is fitted through the collected current/force data. This table shows the linear factor of the fitted lines ( $a$ ).

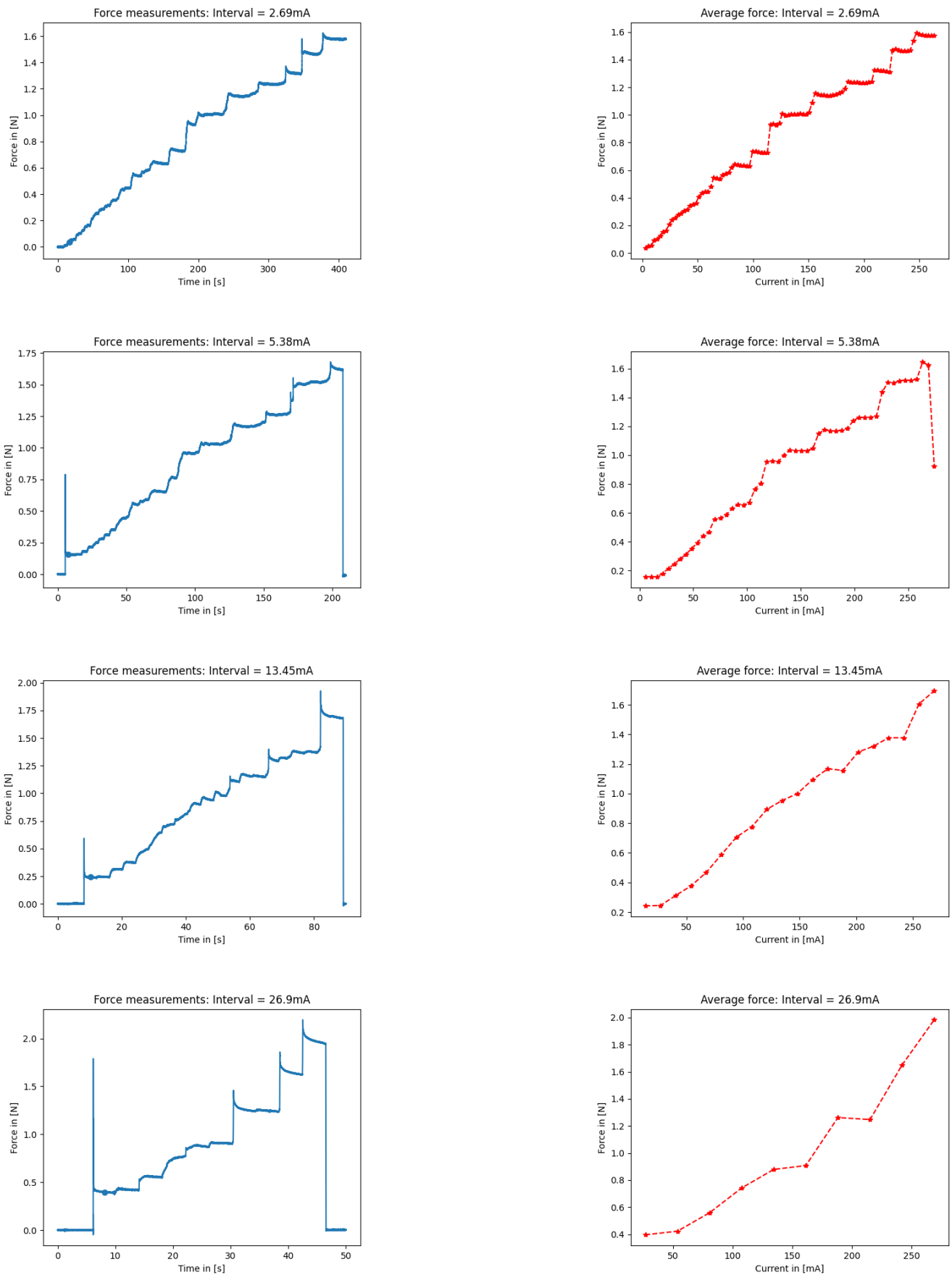


Fig. 4: Force measurements during four different force intervals: 2.69 mA, 5.38 mA, 13.45mA and 26.9mA. Left column: Raw force sensor data. Right column: Average force relative to the applied current.

**APPENDIX B**  
**CHROMATOUGH - DEFORMATION TRACKING**

The ChromaTouch is a tactile sensor which captures deformations. These deformations are used within this research to compute a safety margin. However, other applications could be slip detection, load force detection and shape detection. To capture deformations, the sensor has a silicone dome. This dome is made to be compliant with the object it is touching. Inside the dome, dots are present on the silicone. A camera captures these dots in the core of the sensor.

The sensor is illustrated in Fig. 5a. As can be seen, two layers of coloured dots are present in the silicone dome. These dots enable the image to capture indentation and shear stress on the dome by colour. When the sensor is indented, the dot closest to the sensor surface becomes bigger than the one in front, which causes colour mixing. During shear stress, one dot moves more than the other, which also causes colour mixing (Fig. 5b). In this research, we only look at deformations of the dots by detecting the centre. Therefore the colours of the captured images are not taken into account.

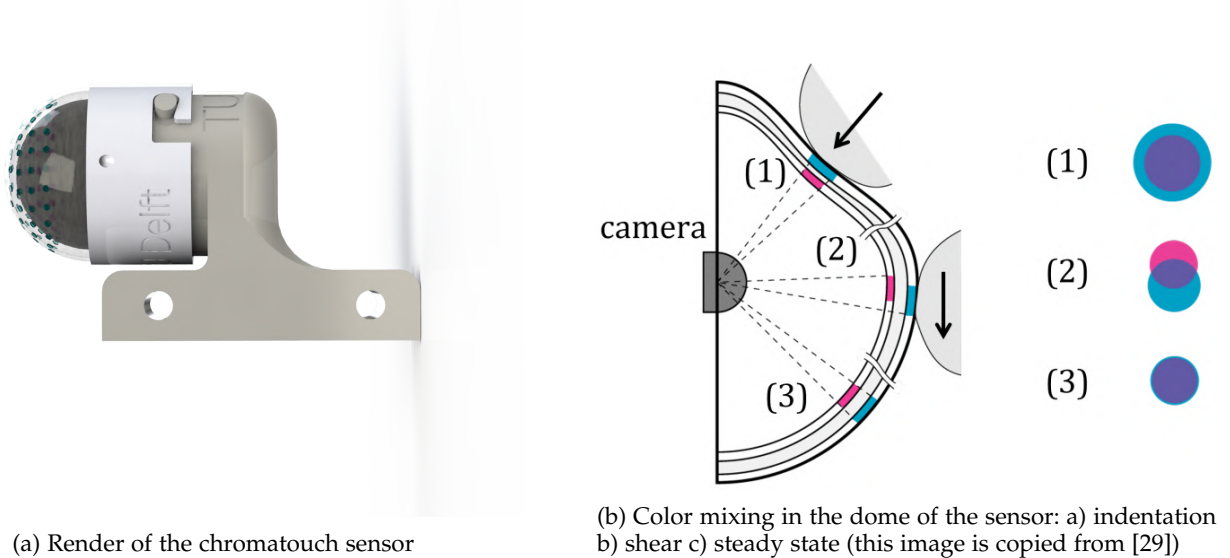


Fig. 5: ChromaTouch sensor

**Deformation detection**

To detect the deformation  $\delta$  in the sensor, first the dots have to be detected. A typical image of the inside of the sensor dome can be seen in Fig. 6a. With OpenCV the dots in the image are detected, see Fig. 6b.

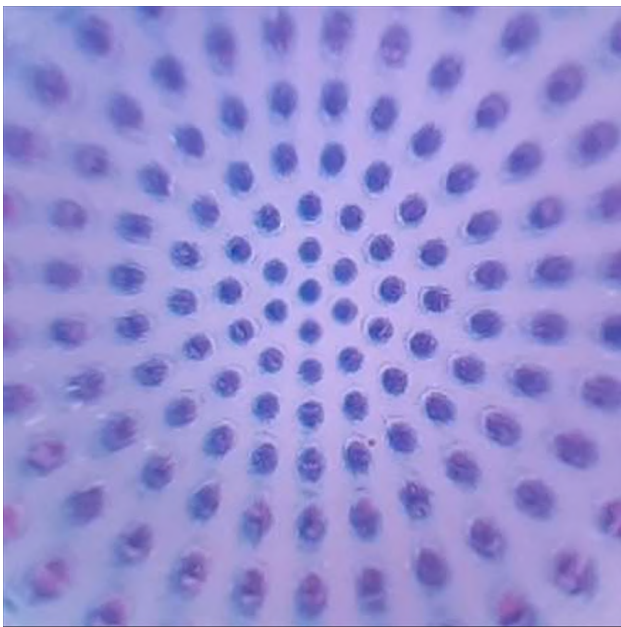
The difference in vertical centre position represents the deformations of the dots over time. However, to do this, we need to know which dot in an image corresponds with the dot of the previous image. Therefore a nearest neighbour algorithm is implemented. When capturing the first image of the inside of the sensor, the user manually detects the centre dot. After this, the nearest neighbour algorithm detects the 20 closest dots.

During all other images, the deformation of the sensor is captured by tracking the centre of the dots. Based on the previously detected 20 dots, the same dot in the new image is detected by the nearest neighbour algorithm. The difference in dot positions between different images gives the deformation (Fig. 7a). The average deformation of the 20 dots is put in a moving time window, with a window of 10, to reduce noise on the output (Fig. 7b).

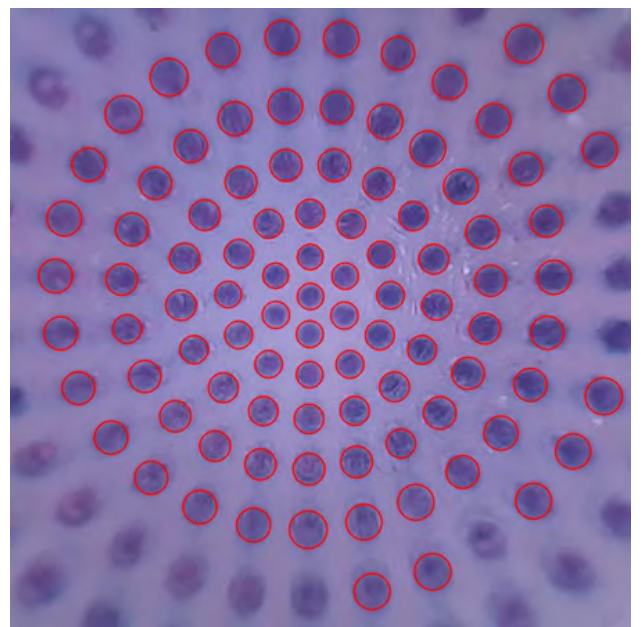
**Future recommendations**

The sensor can detect deformations by the deformability of the sensor dome. However, when the force on the dome has disappeared, the sensor does not return to its initial position in a sufficient time. The sensor needs multiple seconds to return to its initial state, which is very inconvenient when it must sense multiple objects. To improve the return time, we recommend increasing the elasticity of the dome.

We also suggest to improve the deformability of the dome, by adapting the stiffness of the material. Currently, an initial force of 0.6 N is required to detect deformations. This initial force is very inconvenient when touching delicate objects.

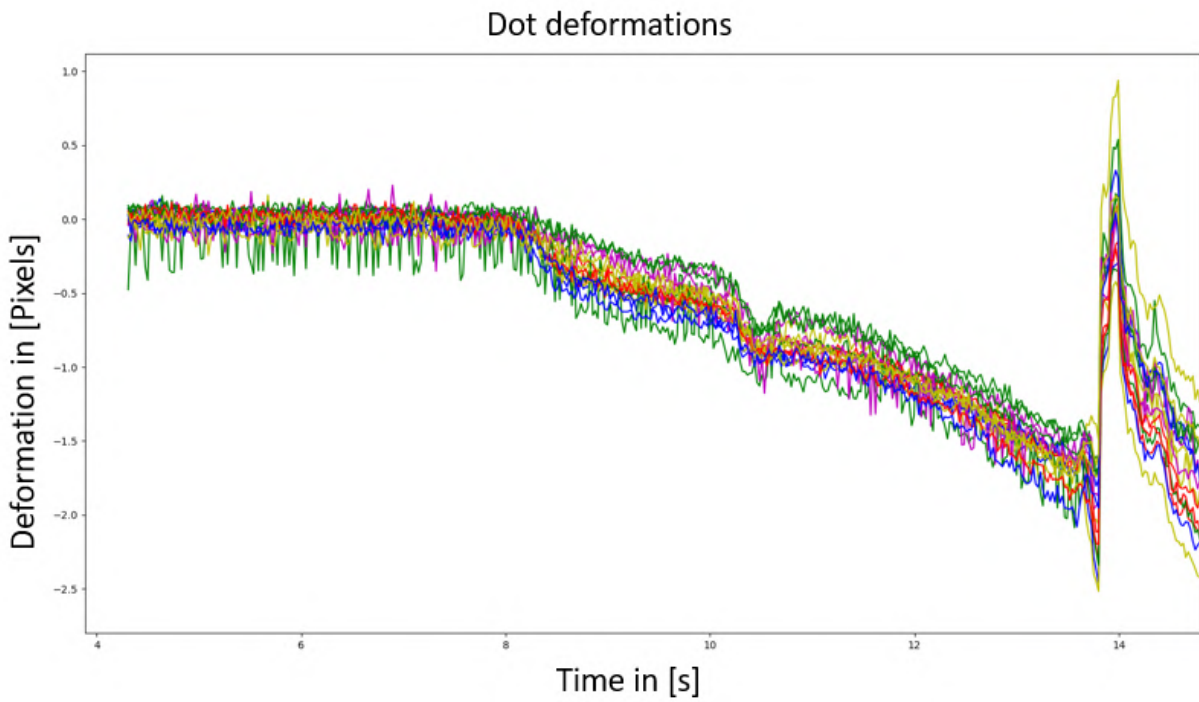


(a) Image of the inside of the sensor

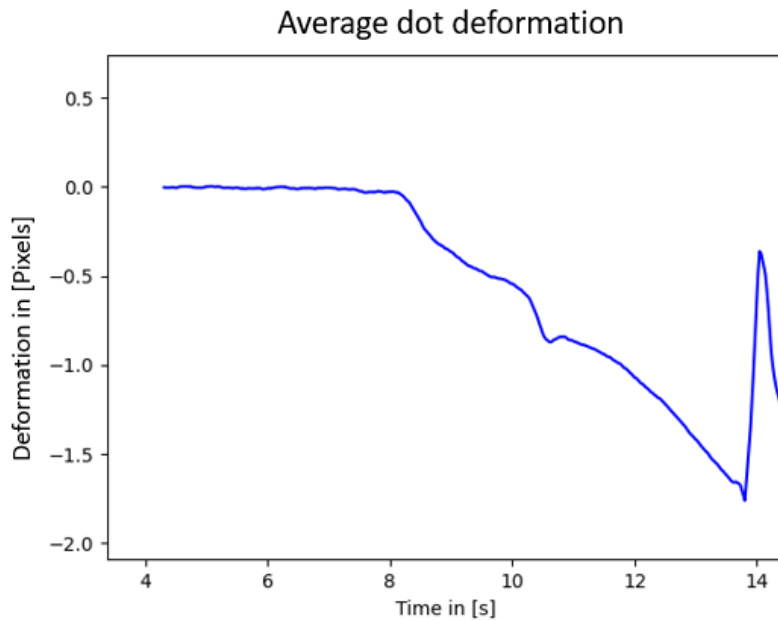


(b) Red circles are dots detected by OpenCV

Fig. 6: Dots inside sensor



(a) Deformation of the 20 most centered dots.



(b) Average deformation in a moving time window of 10 values

Fig. 7: Deformation detection by tracking the dots on the inside of the ChromaTouch.



## APPENDIX C

### CRITICAL DEFORMATIONS

The safety margin is computed based on deformations in the contact area (Equation: 1). To track the deformations in the contact surface, the ChromaTouch is used, as explained in Appendix B.

$$\Gamma = 1 - \frac{\delta}{\delta^*} \quad (1)$$

with  $\Gamma$  the safety margin,  $\delta$  the measured deformation, and  $\delta^*$  the critical deformation

The critical deformation is a pre-determined value and is related to the applied grip force and the object. To find the relation between the grip force and the critical deformation a dataset is collected. This dataset contains the critical deformation for a number of grip forces, by fitting a line through this dataset the relation is found.

#### Data collection

Compiling the dataset of critical deformations is done by the following protocol: The remote gripper grasps an object, and weight is added till the object slips. The deformations of the dots within the sensor show a peak when gross slip is present. This peak is the critical deformation. The critical deformation is collected for 7 different forces ranging from 0.24 to 1.68 N. Per grip force the critical deformation is collected 3 times (Fig. 9). The average of this 3 measurements is used to find the relation between the grip forces and the critical deformation.

#### Relation between the grip force and critical deformation

A Power curve ( $y = ax^b$ ) is fitted through the (average) data to find the relation of the critical deformation per applied grip force (Fig. 8):

$$\delta^* = 2.4585045 \cdot F_{grip}^{2.489725} \quad (2)$$

With  $F_{grip}$  the grip force.

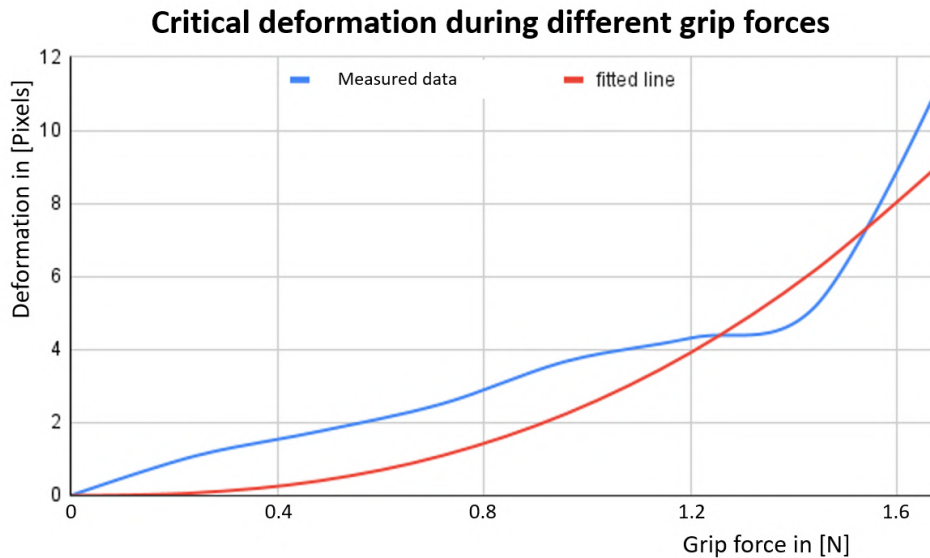


Fig. 8: The relation between the grip force and the critical deformation for a metal can, in blue is the measured data and in red the fitted line.

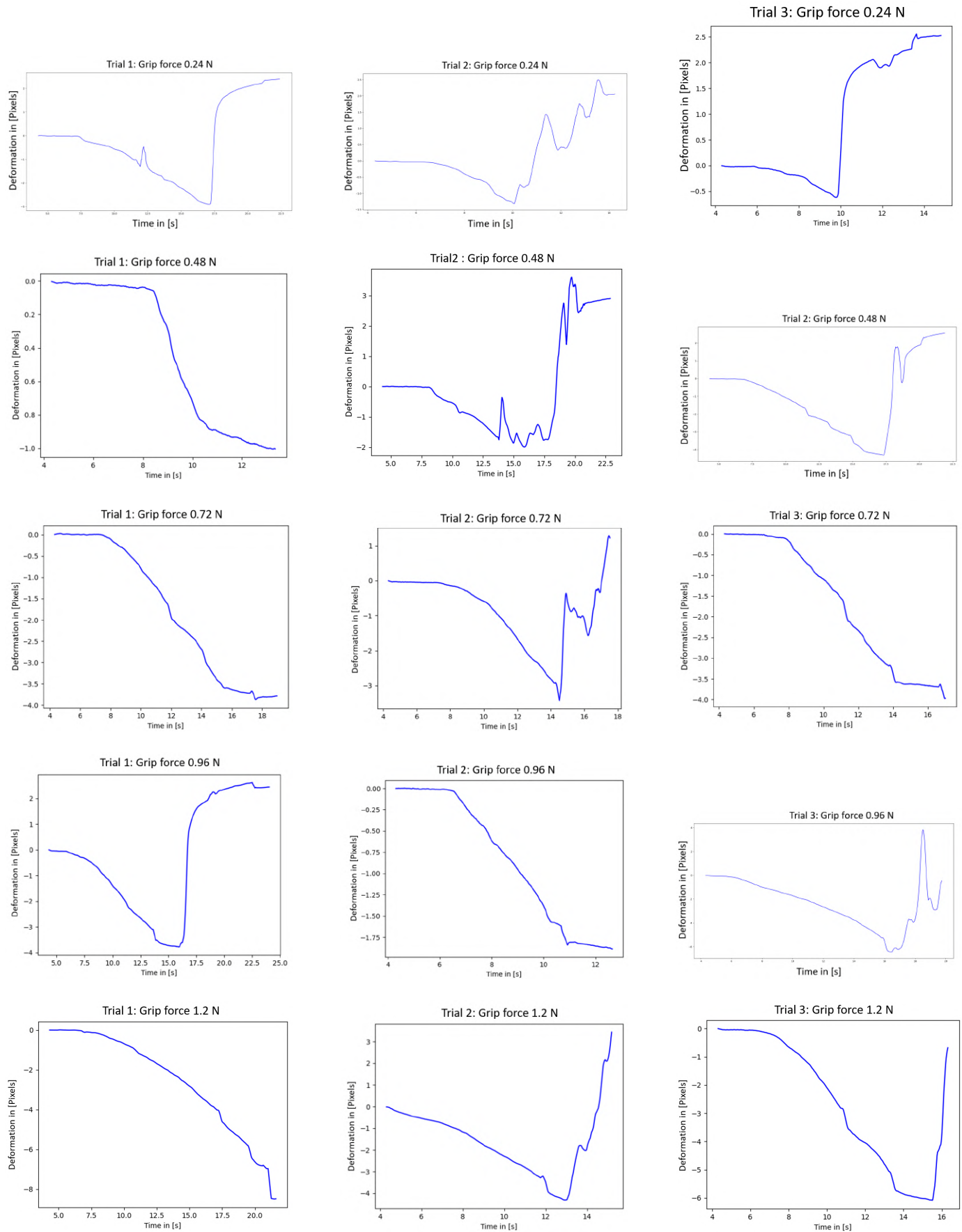


Fig. 9: These figures show the deformation of the contact surface between a metal can and the ChromaTouch sensor while the lateral force increases. The minimum in the figures represents the critical deformation, this is the moment gross slippage occurs. Every row represents a different grip force. (Part 1/2)

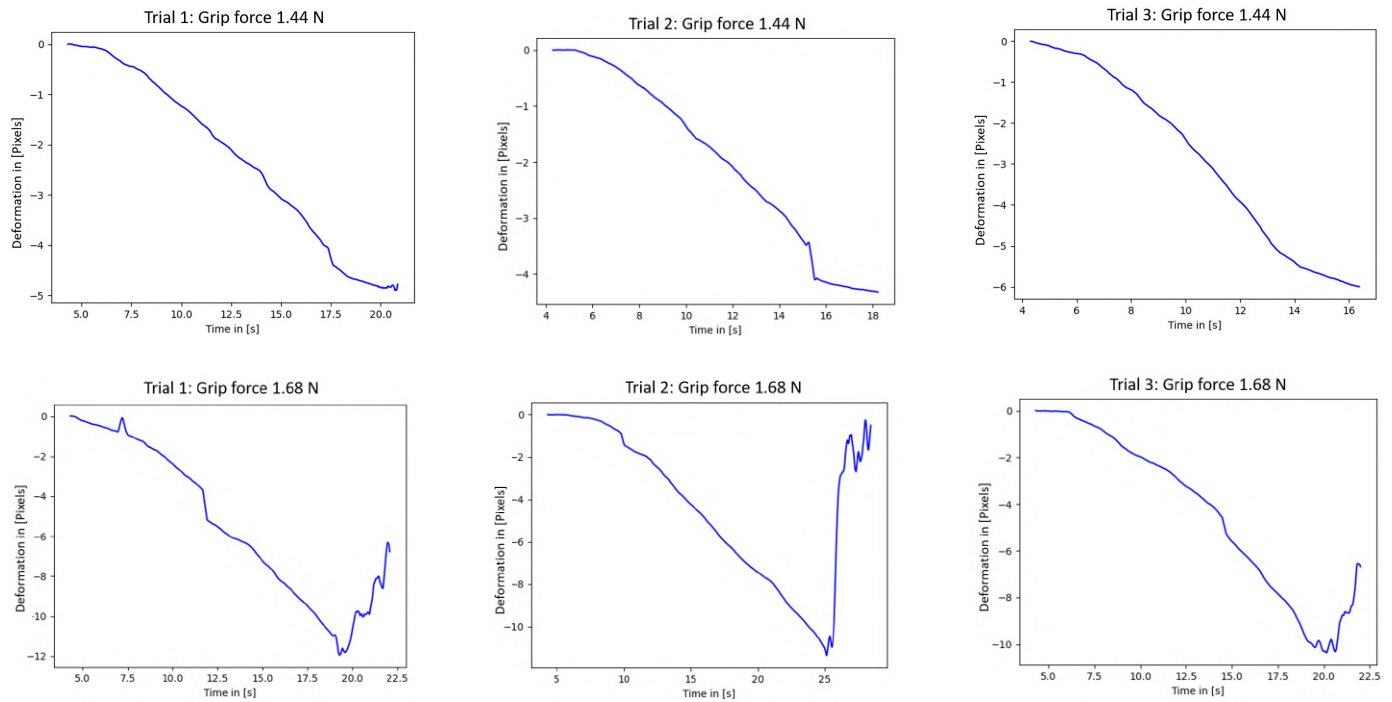


Fig. 9: These figures show the deformation of the contact surface between a metal can and the ChromaTouch sensor while the lateral force increases. The minimum in the figures represents the critical deformation, this is the moment gross slippage occurs. Every row represents a different grip force. (Part 2/2)